first break volume 20.2 February 2002

From seismic to simulator through geostatistical modelling and inversion: Makarem gas accumulation, Sultanate of Oman

G. Shanor, M. Rawanchaikul & M. Sams from Jason Geosystems Middle East and R. Muggli, G. Tiley & J. Ghulam from Petroleum Development Oman discuss how reservoir characterization results achieved with an integrated team effort led to a significant increase in reserves of the Makarem Field, Sultanate of Oman

Introduction

This paper presents an applied workflow and the results of an integrated team effort to define the commercially recoverable reserves associated with the Buah fractured carbonate reservoir of the Makarem sour-gas accumulation in the Sultanate of Oman. The status at the start of the study was that three wells had been drilled into the field, a discovery well Makarem-1 and two exploratory-appraisal wells Makarem-2/-3. Tests of Makarem-1/-3 showed good flow rates, but the Makarem-2 test indicated very tight formation with no flow. The estimated Gas-Initially In-Place (GIIP) volumes based on the assumption of mainly fracture porosity were insufficient to justify field development. The main goal of the study was to determine the potential for significant matrix flow which would be critical to the commerciality of the field.

In this paper we focus on the method applied to develop multiple 3D static model realizations from the available, seismic, well log, geological and engineering information and the use of these models in the assessment of development scenarios. With multiple models available, uncertainty of reservoir parameters determined from static models may be quantified. Further, the P50 model (in terms of volumetrics)

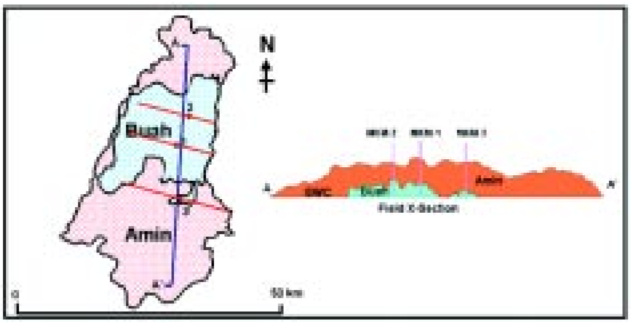

Figure 1 Schematic diagram of the Makarem structure.

was taken into a flow simulator for dynamic modelling to evaluate the potential for matrix flow.

The modelling study confirmed a high likelihood of a sufficient matrix porosity contribution to flow. As a result, Makarem-3 was re-tested specifically to address the fracture/matrix flow transition. The test was successful and proved a significant contribution of the matrix to flow, providing support for the reliability of the models. The reserves proved-up by this exercise form part of the long-term development planning for gas supply in the Sultanate.

Reservoir summary

The Makarem gas discovery is located in the Oman interior in the Block 6 concession and is formed by a large, westward tilted structural high with major N-S trending bounding faults on its eastern side. The structure is situated on the Musallim Slope, a regional high separating the Fahud and Ghaba salt-basins. The crestal part has been partly eroded. Figure 1 shows a schematic diagram of the Makarem structure.

The main reservoir rock in the Makarem structure consists of the Buah Formation of the Nafun Group (Huqf Supergroup). The rock is of Pre-Cambrian age and consists of a sequence of thinly interbedded dolomitized stromatolitic and irregular algal boundstones, oncolitic boundstones, intraclast grainstones, pellet grainstones and mud-wackestones. These carbonates were deposited in a shallow marine to supratidal setting with occasionally short-lived periods of subaerial exposure and desiccation.

The secondary reservoir, the Amin Formation, belongs to the Mahatta Humaid Group (Haima Supergroup) of Cambrian age and consists of medium to coarse-grained fluvial and aeolian sandstones. The Amin is onlapping the underlying Buah Formation.

Both reservoir intervals have proven to be gas bearing by the three wells that have been drilled on the structure so far. Pressure data suggests that both the Amin and the Buah reservoirs form one large accumulation with a single gas column. The ultimate top seal is formed by tight Miqrat mudstones.

The 1996 discovery well, Makarem-1, and the second exploratory-appraisal well Makarem-3 flowed gas from the Buah formation during testing. The first exploratory-appraisal well, Makarem-2 however, penetrated a very tight zone with low flow on test. Fracture porosity is estimated to be around 1%, whereas the reservoir matrix porosity is typically between 0 and 5%. The Amin formation is super tight. The table in Fig. 2 summarizes Makarem reservoir characteristics.

The limited flow in Makarem-2 prompted the need to get a better grip on the uncertainties of the matrix porosity distribution in order to evaluate possible development scenarios.

Methodology

The ultimate goal of the study was to establish that the field contained significant recoverable reserves based on a Unit Technical Cost (UTC) cut-off of $1/Mscf. To leverage available expertise as much as possible a multidisciplinary team staffed with a combination of in-house and external experts was formed to carry out the study. Figure 3 shows an overview of the key information contributions required for this

Reservoir	Amin Sandstone	Buah Dolomite
Group	Palaeozoic Mahatta Humaid	Proterozoic Huqf (Nafun)
Age	Cambrian	Precambrian
Geology	Mixture of fluvial & aeolian deposits from a near source (presence of chert)	Sequence of thinly interbedded dolomitised stromatolitic & irregular algal boundstones, intraclast grainstones, pellet grainstones and mud wackestones deposited in a shallow marine to supratidal setting with occasionally short lived periods of subaerial exposure & desiccation.
Depth	4580 mss	4780 mss
Effective porosity	2–3%	2–4%
Effective permeability	0.02 mD (matrix)	20 mD
Pressure	60 650 kPaa	61 179 kPaa
Temperature	165 °C	168 °C
Gas composition		Dry, H_2S = 4%, CO_2 = 4.5%
Stimulated productivity	25 000 m^3/day	600 000 m^3/day

Figure 2 Makarem reservoir characteristics.

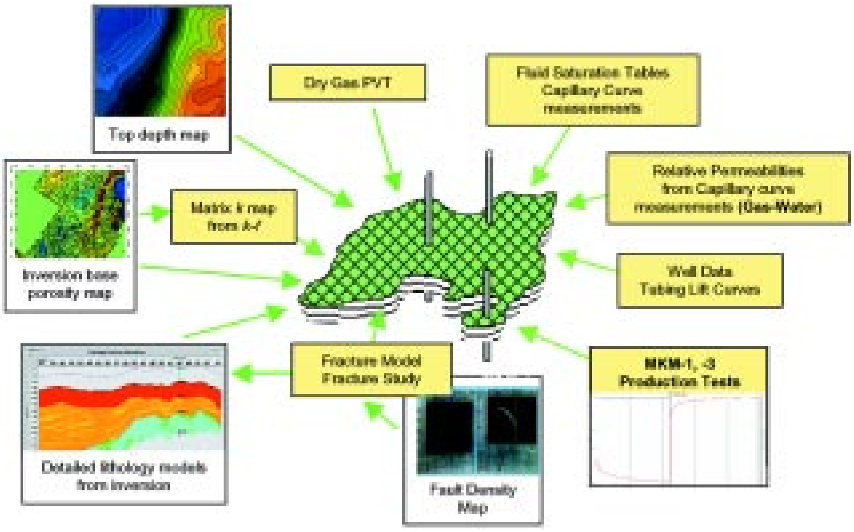

Figure 3 Integrated full field reservoir modelling.

integrated full field reservoir modelling.

Working with acoustic impedance as opposed to seismic amplitude reflection data provides many important interpretive benefits, as discussed in Buxton-Latimer *et al.* (2000). In this study, as a first step in using the seismic data for the reservoir modelling process, an initial acoustic impedance inversion was run with a constrained sparse spike algorithm (Pendrel & Van Riel 1997a). With this method an impedance volume calibrated to well control is generated. Interpretive resolution is enhanced by the conversion from reflection seismic amplitude data to layer acoustic impedance and by broadening bandwidth, on the low frequency side in particular. Figure 4 shows an acoustic impedance section through the well control.

Review of the acoustic impedance (AI) data was encouraging, suggesting a strong relationship between test results and zones of lower impedance associated with higher matrix porosity in the dolomites. The AI volume provides a superior data set for identifying intra-reservoir layers compared with the seismic reflectivity data. The AI volume was used to reinterpret the existing horizon interpretation and to define additional horizons.

The resolution achieved with the constrained sparse spike inversion approach is insufficient for the study's purposes. Much more detailed models are required to characterize the heterogeneity and porosity distribution of the Buah Formation and to determine possible connected matrix porosity volumes. To achieve this, the team turned to a geostatistical inversion methodology that combines seismic inversion with geostatistical modelling. This geostatistical inversion technique builds multiple, equi-probable rock property and lithology models in 3D, which honour all seismic, log and geological input data including the internal stratigraphic framework of each modelled zone.

The main steps in the geostatistical inversion procedure as applied in this study are:

1. Build a stratigraphic framework from selected horizons from the acoustic impedance interpretation. This stratigraphic framework defined the microlayering within each layer defined within the framework, and the stratigraphic layers jointly define a 3D geological model.
2. Perform detailed log analysis to determine lithology at the wells, resulting in a detailed litho-type log at each well.
3. Undertake a geostatistical analysis of the available data to determine variograms of each litho-type within each geological layer in the stratigraphic framework, litho-type probability trends and the distribution of AI in each litho-type.
4. Perform iterative geostatistical litho-type (indicator)

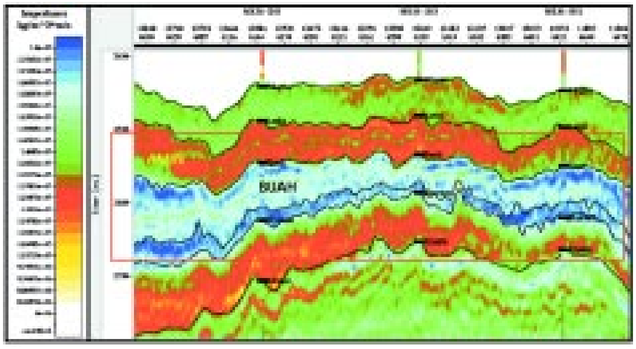

Figure 4 Acoustic impedance section through well control with revised and expanded interpretation.

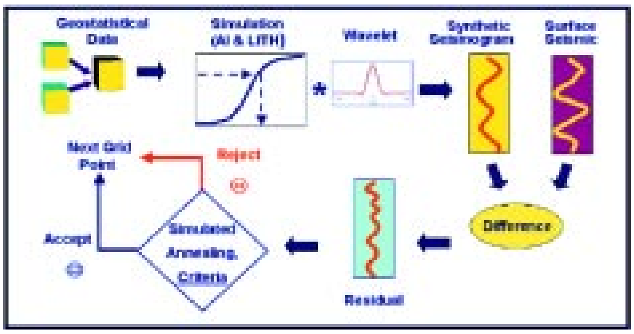

Figure 5 Geostatistical inversion process summary.

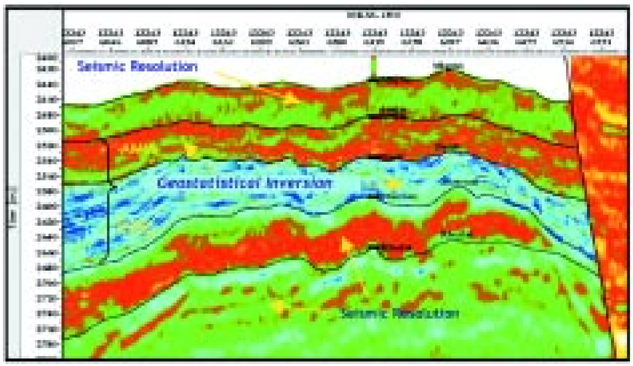

Figure 6 Deterministic and geostatistical inversion merged results

simulation modelling conditioned to the seismic data, as illustrated in Fig. 5. In this step, starting from an initial simulation result, all points in the volume are revisited several times following a random path. At each point litho-type and AI are re-simulated and tested in terms of an improvement of seismic data fit. A new point may then be accepted or rejected based on a simulated annealing criterion, or simply accepted only if the seismic data fit improves.

5 Co-simulate porosity based on a geostatistical analysis of the relationships between the well log porosity, impedance and lithology.

In steps 3, 4 and 5 all spatial processes operate along the microlayers determined from the stratigraphic framework. The process is very robust, and reproduces the seismic data in the time domain as a constraining factor in the inversion process. Torres Verdin *et al.* (1999), Sams (1999) and Pendrel & Van Riel (1997b) provide further examples and more detailed discussions of the methodology. The primary results of this technique are pairs of simultaneously simulated models of acoustic impedance and lithology at essentially any vertical resolution

The geostatistical inversion was carried out at 1 ms resolution (corresponding to 3 m in depth for this study). Figure 6 shows an example highlighting the detailed high-resolution obtained with geostatistical inversion in comparison with deterministic constrained sparse spike inversion at the seismic scale.

Analysis of the relationships between the well log porosity, impedance and lithology provide a geostatistical basis to build parameters for subsequent co-simulation of porosity. The series of models obtained then permits reservoir uncertainties to be quantified.

Results

In this study, five pairs of AI-Litho models resulting from the geostatistical inversion were generated at 1 ms resolution. Figure 7 illustrates results for a set of lines through the well control.

Upon completion of the lithology/AI simulation, three porosity models were co-simulated from each of the five AI-Lithology models. This results in a total of 15 porosity models to characterize and quantify the Buah reservoir heterogeneity and porosity distributions and to allow assessment of connectivity. Based on the 15 porosity models, along with the water contacts and velocity models for time-depth conversion, volumetric computations were performed on each model, so allowing ranking of the realizations. As an example, the P50 net

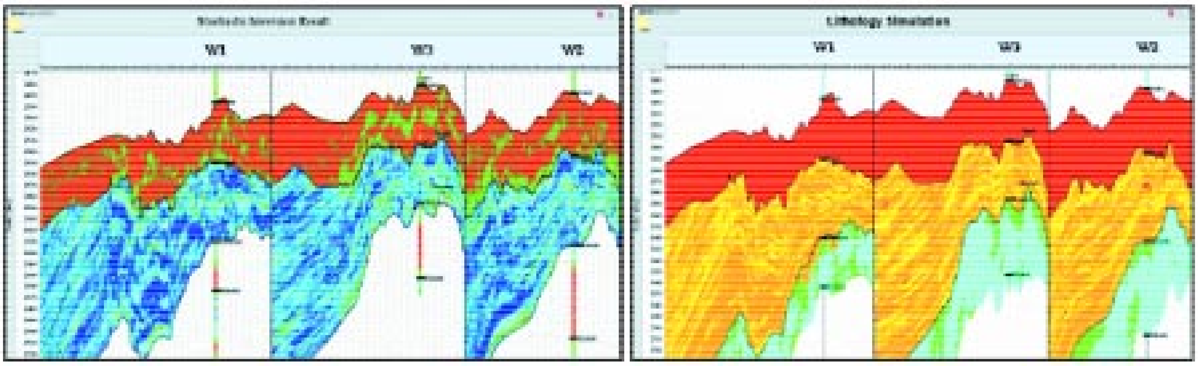

Figure 7 One pair of 1 ms vertical resolution acoustic impedance and lithology models. Lines of section are shown in Fig. 1 as red lines through the wells.

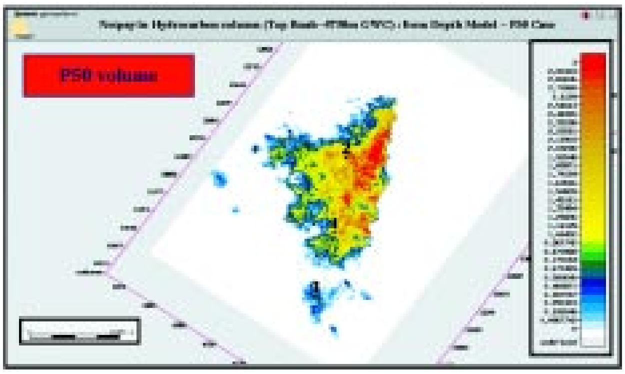

Figure 8 The hydrocarbon net pay map for the P50 model using a 2% porosity cut-off.

pay map is shown in Fig. 8. These results indicate that the modelled range of connected Buah matrix porosity is significant, as compared with the assumed 1% fracture porosity alone. This justified the re-test and stimulation of Makarem-3 with the specific objective of seeing the fracture-matrix flow.

For purposes of reserves booking, the mean case (P50) porosity model derived from the geostatistical inversion has been used as the basis for building a reservoir simulation model. After depth conversion of the model, the first step was to reduce the huge amount of data (56 million cells) to less than 4 million cells by upscaling spatially from the 75 × 75 m geostatistical inversion and simulation output grid to a 300 × 300 m grid, while maintaining the modelled vertical resolution of 3 m. A cross-section through the simulation model is shown in Fig. 9.

This model was then integrated with production data obtained from capillary curve measurements and a fracture porosity model. The well trajectories (horizontal and vertical) used in the dynamic model for evaluating the production potential have been targeted at the porosity sweet spots using a well bore trajectory planning tool operating on the full resolution (56 m cells) model. Figure 10 shows a well planning example.

The dynamic reservoir simulation results show that the modelled matrix porosity and associated permeability contributes to a significant increase in the producible gas volumes in the Buah reservoir. This result has been confirmed by the successful conclusion of the re-tested well, as discussed by Al Ghulam (2001) and Jones (2001), further confirming the validity of the models. The increase in producible reserves and the matrix porosity contribution to flow determined by the geostatistical inversion and dynamic reservoir modelling has justified the booking of significant additional reserves.

Conclusions

The reservoir characterization results achieved with an integrated team effort have led to a step change in the understanding of the Makarem Field. One key component of the study involved bringing in seismic information to help determine the spatial distribution of matrix and fracture porosity in the carbonate Buah formation. The seismic information was brought in through geostatistical inverse modelling and simulation, resulting in detailed lithotype/porosity models. To complete the 'Seismic to Simulator' workflow the P50 model was brought into a reservoir simulator for detailed flow modelling.

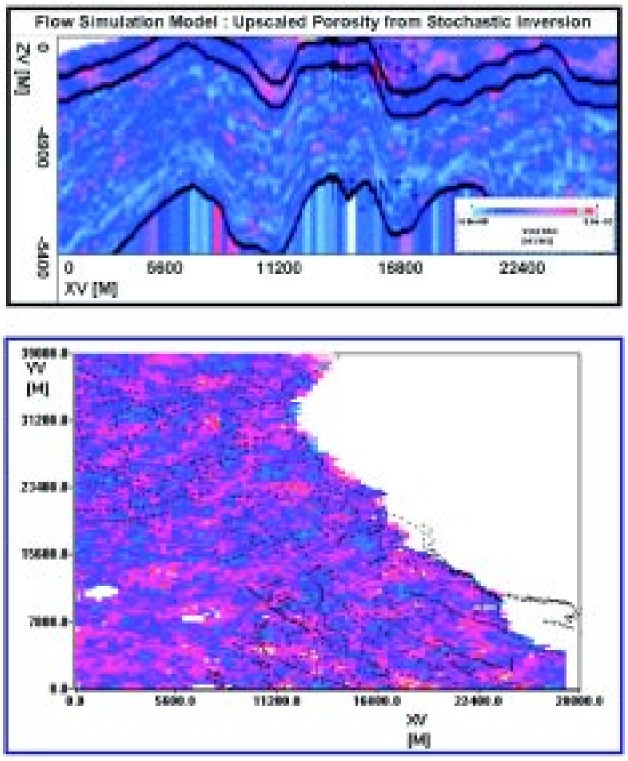

Figure 9 The P50 upscaled porosity model from geostatistical inversion in the reservoir simulator. Section view and map of the top Buah layer

As demonstrated, geostatistical inverse modelling and simulation provides a robust engine to quantitatively integrate well log, geological, engineering and seismic information. The generation of multiple realizations at high resolution (1 ms in seismic time or 3 m in depth for this study) over the full reservoir area supported the assessment of uncertainty in the volumetric estimates and selection of a model to take forward into the dynamic reservoir simulation phase of the study.

The generated porosity models have indicated good development of matrix porosity in the field. The re-test of Makarem-3 and flow simulation modelling has confirmed that the modelled levels of matrix porosity and associated permeability support production.

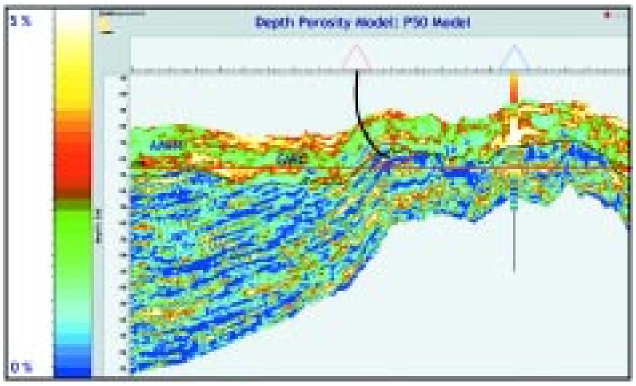

Figure 10 Example of well planning targeting the high porosity reservoir sweet spots.

These studies have resulted in a substantial increase in the initial estimates of potentially producible reserves at Buah level. Further work is necessary to address in full detail the inherent risks associated with producing sour (H_2S rich) gas and its potential impact on health, safety and environment. The sour gas nature of the Buah accumulation will have a major influence on the timing of its development.

Acknowledgements

The authors would like to thank the Ministry of Oil and Gas in the Sultanate of Oman for permission to present this workflow and results.

References

Al Ghulam, J., Al Shidi, S. & Mazarett, P. [2001] Makarem: a Recipe for Testing the Limits in Central Oman Gas Exploration. Paper SPE 68138, prepared for the *12th Middle East Oil Show and Conference*, Bahrain, March 2001.

Buxton-Latimer, R., Davison, R. and Van Riel, P. [2000] An interpreter's guide to understanding and working with seismic-derived acoustic impedance data. *The Leading Edge* **March**.

Jones, A., Rodenboog, C., Hill, D., Anwar H., Akbar A. and de Boer, P. [2001] An engineered approach to matrix acidizing HTHP sour carbonate reservoirs. Paper SPE 68915, prepared for the *SPE European Formation Damage Conference*, The Hague, Netherlands, 21–22 May 2001.

Pendrel, J. and Van Riel, P. [1997a] Methodology for seismic inversion and modeling: a Western Canadian reef example. *CSEG Recorder,* **12**(5), 5–15.

Pendrel, J. and Van Riel, P. [1997b] Using seismic inversion and geostatistics to estimate porosity: A Western Canadian reef example, *CSEG Annual Meeting*, 1997.

Sams, M.S., Atkins, D., Said, N., Parwito, E. and Van Riel, P. [1999] Stochastic inversion for high resolution reservoir characterization in the central Sumatra basin, SPE 57260. Presentation at the *1999 SPE Asia Pacific Improved Oil Recovery Conference*, Kuala Lumpur, Malaysia.

Torres Verdin, C., Victoria, M., Merletti, G. and Pendrel, P., [1999] Trace based and geostatistical inversion of 3D seismic data for thin sand delineation: an application to San Jorge Basin, Argentina. *The Leading Edge* **September**.